



HAL
open science

Molecular Electrochemical Reductive Splitting of Dinitrogen with a Molybdenum Complex

Lydia Merakeb, Soukaina Bennaamane, Jérémy de Freitas, Eric Clot, Nicolas Mézailles, Marc Robert

► **To cite this version:**

Lydia Merakeb, Soukaina Bennaamane, Jérémy de Freitas, Eric Clot, Nicolas Mézailles, et al.. Molecular Electrochemical Reductive Splitting of Dinitrogen with a Molybdenum Complex. *Angewandte Chemie International Edition*, In press, 7 p. 10.1002/anie.202209899 . hal-03758536

HAL Id: hal-03758536

<https://hal.science/hal-03758536v1>

Submitted on 23 Aug 2022

HAL is a multi-disciplinary open access archive for the deposit and dissemination of scientific research documents, whether they are published or not. The documents may come from teaching and research institutions in France or abroad, or from public or private research centers.

L'archive ouverte pluridisciplinaire **HAL**, est destinée au dépôt et à la diffusion de documents scientifiques de niveau recherche, publiés ou non, émanant des établissements d'enseignement et de recherche français ou étrangers, des laboratoires publics ou privés.

Molecular Electrochemical Reductive Splitting of Dinitrogen with a Molybdenum Complex

Lydia Merakeb,^[a] Soukaina Bennaamane,^[b] Jérémy De Freitas,^[a] Eric Clot,^[c] Nicolas Mézailles,^{*[b]} and Marc Robert^{*[a][d]}

[a] Dr. L. Merakeb, Jérémy De Freitas, Prof. M. Robert
Laboratoire d'Electrochimie Moléculaire – UMR 7591
Université de Paris
15, rue Jean Antoine de Baïf 75013 Paris, France
E-mail: robert@u-paris

[b] Dr. S. Bennaamane, Dr. N. Mézailles
Laboratoire Hétérochimie Fondamentale et Appliquée – UMR 5069
Université Toulouse III – Paul Sabatier
118, route de Narbonne, Bât 2R1, 31062, Toulouse, France
E-mail: mezaillies@chimie.ups-tlse.fr

[c] Dr. E. Clot
ICGM
Univ Montpellier, CNRS, ENSCM
Montpellier, France

[d] Prof. M. Robert
Institut Universitaire de France (IUF)
F-75005, Paris, France

Supporting information for this article is given via a link at the end of the document.

Abstract: Nitrogen reduction in mild conditions (*i.e.*, room T and atmospheric P), using a non-fossil source of hydrogen remains a chemistry challenge. Molecular metal complexes, notably Mo based, have recently shown to be active for such nitrogen fixation. In this work, we report about the electrochemical N_2 splitting with Mo^{III} triphosphino complex [(PPP)Mo]₃, at room temperature and a moderately negative potential. A Mo^{IV} nitride species was generated, which was confirmed by electrochemistry and NMR studies. The reaction goes through two successive one electron reduction of the starting Mo species, coordination of an N_2 molecule, and further splitting to a Mo^{IV} nitride complex. Preliminary DFT investigation supports the intermediacy of a bridging Mo/N_2Mo' dinitrogen dimer evolving to the Mo nitride via a low energy transition state. This example joins a short list of molecular electrochemical complexes for N_2 reductive cleavage. It opens a door to molecular electrochemical PCET conversion studies of N_2 to NH_3 .

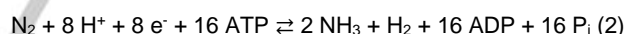
Nitrogen is one of the essential elements for life.^[1] Although abundant, it is nonetheless a limiting nutrient in agriculture, and crops growth is dependent on its availability.^[2] It is not only essential to the global economy as a fertilizer but also as the feedstock for industrial production of all N containing derivatives. Moreover, it has been identified as an alternative fuel as well as an energy storage molecule.^[3,4] Today, ca. 200 million tons of NH_3 are produced yearly, exclusively by the Haber-Bosch (H-B) process (equation (1)).



Although thermodynamically favorable, the reaction is carried out at high temperature (300 - 500 °C) and high pressure (200 - 300 bars) conditions over heterogeneous Fe containing catalysts, using ca. 1 - 2% of the global energy production. It generates half a Gigaton of CO_2 /year (*ca.* ½ of the CO_2 generated is due to H_2 production by CH_4 reforming), a giant carbon footprint.

Nature, by means of microorganisms, transforms N_2 into NH_3 under ambient conditions, via multiple proton/electron transfers.^[5]

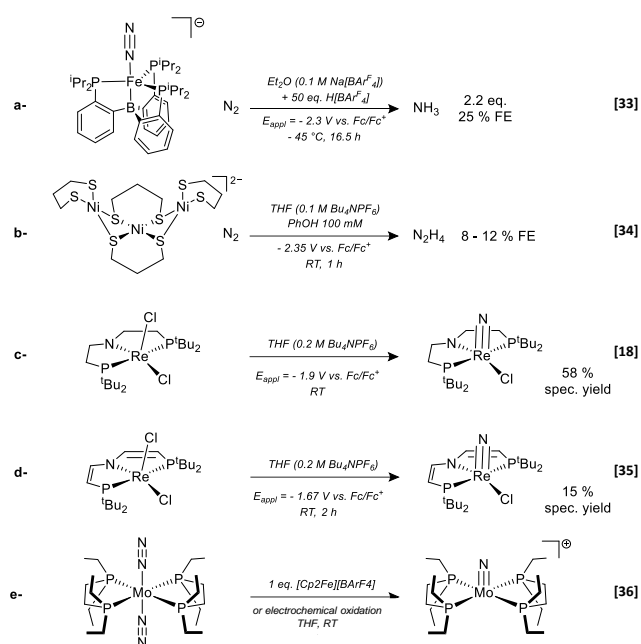
Nitrogenase enzymes, responsible for this " N_2 fixation" reaction (equation (2)), contain an organometallic active site, a $MoFe_7S_9C$ -homocitrate cluster for the most common nitrogenase, which can be viewed as a homogeneous catalyst. The fact that this catalyst involves a coordination/activation of N_2 at one/several metal centers has spurred "organometallic chemists" to search for homogeneous catalysts able to achieve the N_2 -to- NH_3 reaction efficiently.



Transition metal complexes based on Mo^[6-12] and Fe^[13-16], mainly, but also rhenium^[17-19], vanadium^[20], chromium^[21-23], cobalt^[24,25] and titanium^[26] have been investigated in this purpose. However, a major hurdle toward such chemistry lies in the kinetically favorable proton reduction into H_2 . Thus, despite several decades of active research, only a handful of catalysts are known for this reaction. Regarding electrochemical nitrogen splitting with molecular complexes,^[27-29] an early example was identified by Picket and Talarmin with a W complex,^[30] and in recent years, work has been performed on Ti^[31] and Al^[32] based complexes as well. So far, the first example of electrochemically driven N_2 -to- NH_3 catalytic conversion with a well-defined molecular species was reported in 2016. $P_3^B Fe(N_2)$ - (P_3^B = tris(*o*-diisopropylphosphinophenyl)borane) converts N_2 to NH_3 in Et_2O containing 0.1 M $Na[BAr^F_4]$ as a supporting electrolyte (BAr^F_4 = tetrakis(3,5-bis(trifluoromethyl)phenyl)borate) at -45 °C (Scheme 1a). With 50 eq. of $H[BAr^F_4]$ as a proton source and upon applying

COMMUNICATION

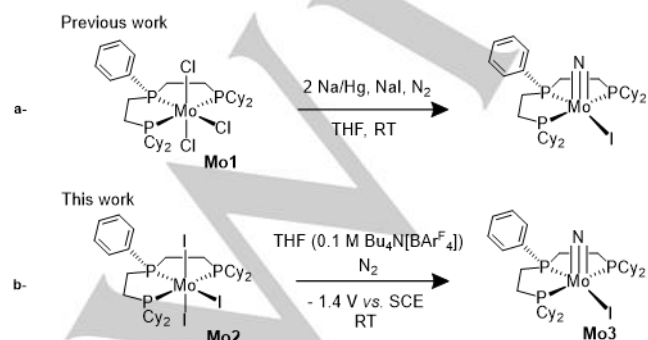
a potential of -2.3 V vs. Fc/Fc^+ , 2.2 eq. of ammonia were produced with 25 % Faradaic efficiency over 16.5 h.^[33]



Scheme 1. Previous examples of molecular electrochemical reduction of N_2 to NH_3 (a), hydrazine (b) or nitride complexes (c-e).

Recently, partial electrochemical reduction of N_2 to hydrazine was shown at a tri-nickel based molecular catalyst. In THF (0.1 M Bu_4NPF_6), N_2 was converted into N_2H_4 at -2.35 V vs. Fc/Fc^+ with 8 to 12 % Faradaic efficiency, in the presence of 0.1 M phenol as a proton source (Scheme 1b).^[34] Most recently, Peters demonstrated tandem electrochemical PCET (proton-coupled electron transfer) for N_2 reduction reaction. Using a cobalt PCET mediator and Pickett's $[\text{W}(\text{dppe})_2(\text{N}_2)_2]$ complex, N_2 was converted to up to 11.5 equiv. of NH_3 at -1.35 V vs Fc/Fc^+ with 45% FE (100 eq. TsOH as proton source, in DME).^[35]

Electrochemical N_2 activation through splitting of the triple bond into metal nitrides has been recently the focus of several studies. Schneider, Siewert et al.^[18] have used a Re^{III} complex for electrochemical conversion into Re^{V} -nitride in 58 % yield at $E = -1.9$ V vs. Fc/Fc^+ in presence of dinitrogen (Scheme 1c). Using a rhenium complex with a similar but more conjugated pincer ligand led to N_2 splitting at a less cathodic potential, however at the



Scheme 2. Molybdenum complex for N_2 splitting in chemical (a) and electrochemical (b) conditions.

expense of a lower yield (Scheme 1d).^[36] Masuda *et al.* showed that splitting of dinitrogen into terminal nitrides is also possible by chemical and electrochemical oxidation of a N_2 -bound Mo^0 complex (Scheme 1e).^[37] Still regarding molybdenum, we have shown that the splitting of N_2 could be achieved through the two electron reduction of a (PPP) MoCl_3 complex (Scheme 2a) in the presence of NaI , and subsequently studied the functionalization of the nitride complex by silanes and boranes.^[10]

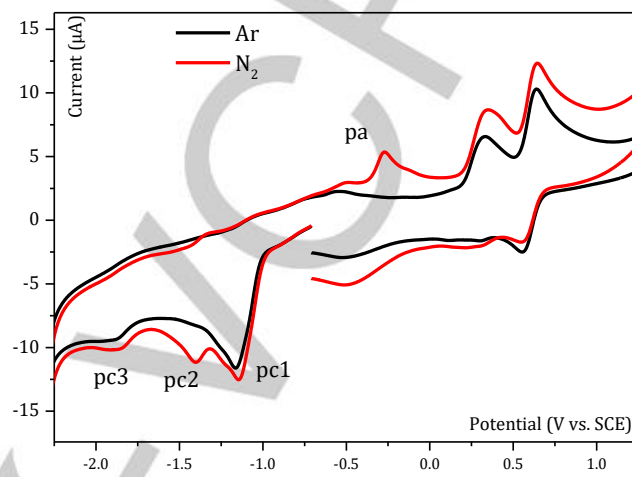


Figure 1. CVs of **Mo2** (0.58 mM) in THF + 0.1 M $\text{Bu}_4\text{N}[\text{BAF}_4]$ at a glassy carbon electrode, under Ar (black) and N_2 (red), at $v = 100$ mV/s and room temperature (RT). The initial potential was set at a value of -0.75 V vs SCE and the scan started toward reduction.

These experimental studies, coupled to DFT calculations demonstrated the possible transformation of the nitride to imido (boryl and silyl) and to amido derivatives, which are related to the key intermediates toward complete reduction to ammonia.^[38] In this work, we achieved the electrochemical splitting of dinitrogen with a Mo^{III} tris-phosphino complex (PPP) MoI_3 (**Mo2**, Scheme 2b) that leads to the formation of the corresponding Mo -nitride complex, at room temperature and moderate potential.

The cyclic voltammetry of **Mo2** was performed in THF and in chlorobenzene, showing similar behaviour (Figures 1 and 2, respectively). Under Ar, it shows four distinct features. As seen for example in THF (Figure 1), a first reduction wave was observed at -1.15 V vs. SCE. Comparison to reversible couple of similar size shows that reduction is mono-electronic (ESI, Figure S6). It was further confirmed upon electrolysis experiment under Ar that the wave involves one electron exchange (ESI, Figure S9). It could thus be assigned to $\text{Mo}^{\text{III}}/\text{Mo}^{\text{II}}$ couple.

COMMUNICATION

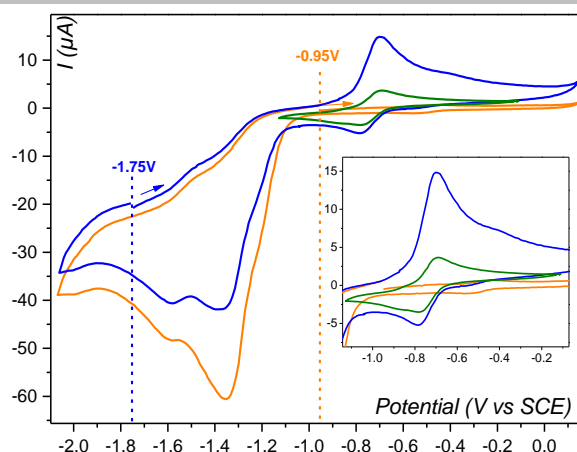


Figure 2. CVs of **Mo2** (4.4 mM) in THF + 0.1 M $\text{Bu}_4\text{N}[\text{BARF}_4]$ under N_2 atm, at $v = 100$ mV/s and RT. The starting potential, indicated with an arrow, was held for 15 s (orange and blue). Green trace: CV of **Mo3** (1.08 mM) in THF + 0.1 M $\text{Bu}_4\text{N}[\text{BARF}_4]$ under N_2 atm., at $v = 100$ mV/s, RT. Inset: zoomed view of the CV in the potential window where **Mo3** is oxidized.

Irreversibility of this wave (observed even at high scan rate) may be ascribed to a chemical step following the initial electron transfer, most likely iodide ligand dissociation. Indeed, oxidation waves at ca. 0.35 and 0.62 V (E^0 , reversible) vs. SCE are observed, corresponding to I^- oxidation to I_2 and I_3^- respectively (see Figure S13). A second irreversible wave is located at -1.8 V vs. SCE (Figure 1, pc3). It may be noted that great care should be taken in the choice of supporting electrolyte anion. The classical hexafluorophosphate (PF_6^-) does coordinate to Mo, preventing any further reactivity with N_2 (ESI, Figure S5). The bulky, non-coordinating tetrakis(3,5-bis(trifluoromethyl)phenyl)borate (BARF_4^-) should be preferred.

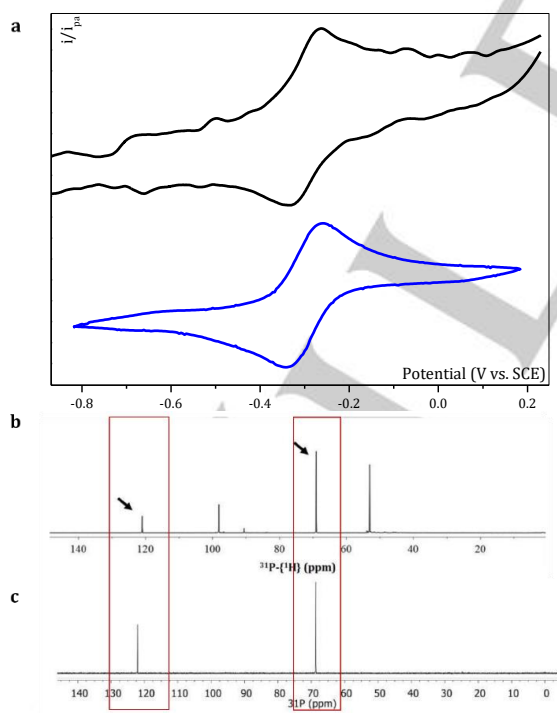
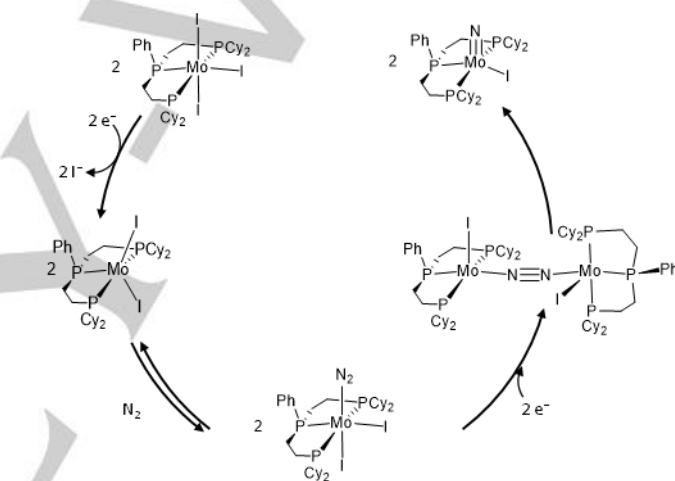


Figure 3. a) CV at 1 mm GC disk of the electrolyte solution after CPE (black) of **Mo2** (2.46 mM) and CV at 3 mm GC disk of **Mo3** (1.12 mM) in THF + 0.1 M $\text{Bu}_4\text{N}[\text{BARF}_4]$ under N_2 atm., at $v = 100$ mV/s, RT. b) $^{31}\text{P}\{^1\text{H}\}$ NMR of the same electrolyte solution. c) $^{31}\text{P}\{^1\text{H}\}$ NMR of complex **Mo3** in THF- d_8 .

Under an atmosphere of N_2 , the cyclic voltammetry of **Mo2** shows additional features. A new reduction peak appears at -1.40 V vs. SCE in THF (Figure 1, pc2), along with a related oxidation peak at -0.26 V vs. SCE (Figure 1, pa). This later peak is only observed when the potential is scanned until pc2, thus it corresponds to the oxidation of a species formed at this later wave. Both waves are diffusion limited. The intensity of the first reduction peak (Figure 1, pc1) increases slightly and the peak potential is positively shifted under N_2 , suggesting possible coordination to dinitrogen. The initial electrochemical behavior could be restored upon Ar bubbling.

The irreversible pc3 wave is not affected by the presence of N_2 . We hypothesized that it could be due to the reduction of a small amount of Mo-oxo complex $[(\text{PPP})\text{Mo}=\text{O}(\text{I})_2]$. Indeed, an authentic sample of the synthesized oxo complex gave a CV reductive signal at similar potential than pc3 (Figure S14) and ^{31}P -NMR confirmed the presence of a small quantity of the oxo species (two singlet peaks at 47 and 95 ppm), typically a few



Scheme 3. Plausible mechanism for electrochemical reduction of N_2 with **Mo2** complex.

percent of the initial complex. Its presence may be due to traces of oxygen or water, or impurity. Likewise, NMR analysis after electrolysis (see below) does show an increase of the oxo complex signal (typically from ca. 3% to 13%, quantified by comparison with PPh_3 as an internal standard). The reduction of **Mo2** in chlorobenzene as solvent, also gives a reduction wave similar to pc3 due to the initial small amount of oxo species (Figure 2; note that redox waves are shifted to more negative potentials as compared to THF). In this solvent, electrolysis does not lead to an increase of the oxo concentration. Focusing on the species formed at wave pc2 and oxidized at wave pa, CVs of an authentic sample of **Mo3** were recorded in the same conditions. Oxidation of this complex occurs at the exact same potential as the species formed at pc2, as shown in Figure 2 and Figure S15, recorded in chlorobenzene and in THF respectively.

This indicates the likely formation of the nitride complex **Mo3** at pc2 reductive wave. To further investigate and demonstrate N_2 reductive splitting, a controlled potential electrolysis (CPE) of a THF solution (+ 0.1 M $\text{Bu}_4\text{N}[\text{BARF}_4]$) containing **Mo2** and saturated with N_2 was performed at -1.4 V vs. SCE, i.e. at pc2 peak

COMMUNICATION

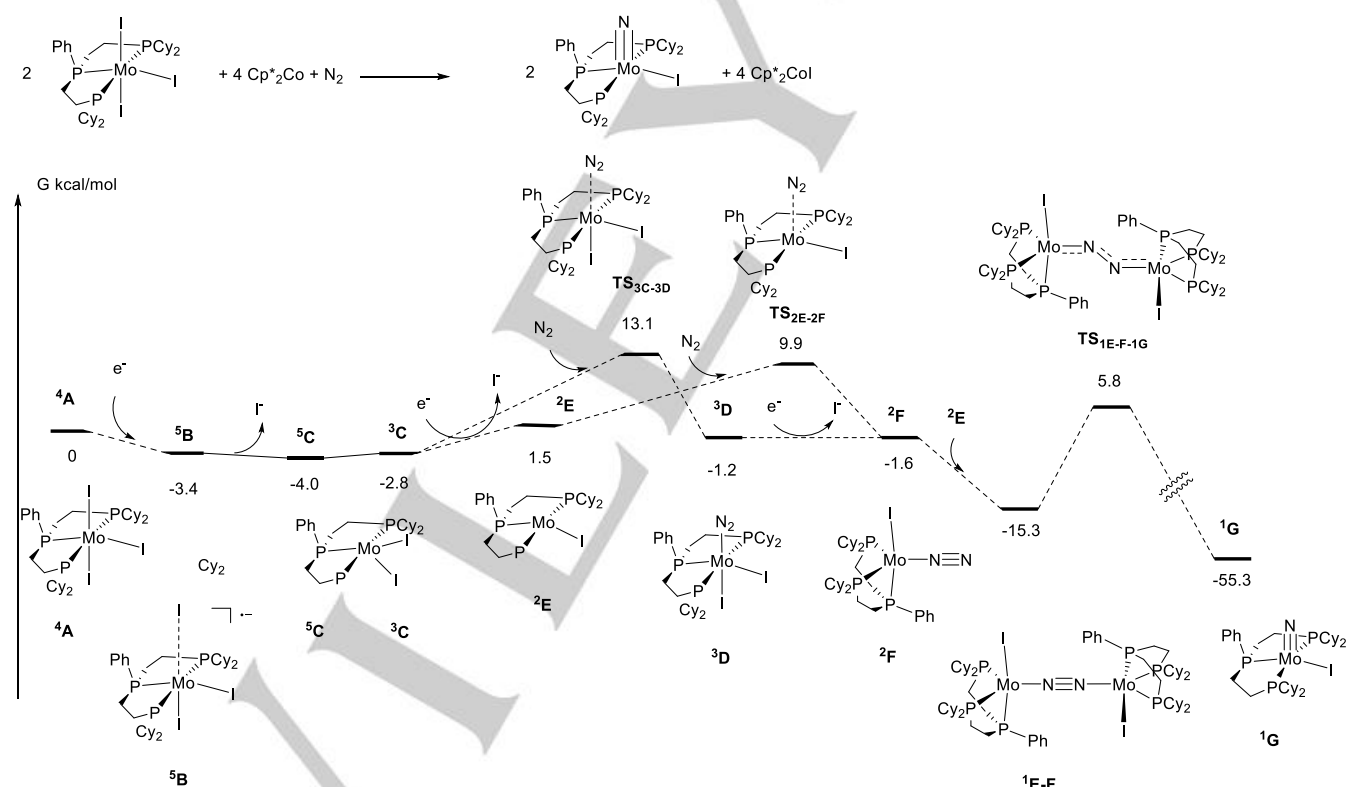
potential. After a few minutes, coloration of the electrolyte solution changed from orange to greenish. After 35 min, a charge of 1.03 C was exchanged, corresponding to 1.24 e⁻ per Mo centre (see ESI for details). At the end of the electrolysis, cyclic voltammetry of the electrolyte solution was performed. The oxidation waves observed at ca. 0.5 and 0.75 V vs. SCE correspond to oxidation of iodide ions to I₂ and I₃⁻ along with a reduction wave at ca. -1.75 V vs. SCE, corresponding to the pc3 wave. Most importantly, a new reversible wave is observed at -0.31 V vs. SCE (Figure 3a). This wave corresponds to the reversible oxidation of Mo^{IV} nitride complex **Mo3**, electrochemically generated during the CPE. Indeed, comparison with CVs of an authentic sample of **Mo3** yields a reversible wave at the exact same potential (Figure 3a). ³¹P-NMR provided further characterization of the nitride complex. [39] After the CPE, the electrolyte solution was concentrated in a J-Young NMR tube, and a small volume of deuterated THF was added. Figure 3b shows two singlet peaks at 69 and 121 ppm respectively, which are characteristic of complex **Mo3** as deduced from comparison with the ³¹P{¹H} spectrum of an authentic sample **Mo3**. The two additional singlet peaks observed at 53 and 98 ppm correspond to the signal of oxo species, as already discussed.

When the electrolysis experiment was performed under an Ar atmosphere, **Mo3** complex was not formed, as neither the reversible wave at -0.31 V vs. SCE in cyclic voltammetry, nor the

signals at 69 and 121 ppm in ³¹P{¹H} NMR were observed. Similar results were obtained in chlorobenzene under both Ar and N₂.

Combined CV and ³¹P NMR data converge to the robust conclusion that **Mo3** is obtained from **Mo2** and dinitrogen upon electrochemical reduction. The chemical yield of the reaction could be derived from cyclic voltammetry by comparing the intensity of the observed reversible wave at -0.31 V after CPE with a CV recorded in the same electrolyte conditions, before CPE. The chemical yield was thus found to be ca. 30 % based on the Mo. Since the charge passed during the electrolysis was 1.24 e⁻ per Mo, less than the 2 e⁻/Mo required for the full conversion of **Mo2** to **Mo3**, the Faradaic yield for **Mo3** production is equal to 49%. The fact that **Mo2** is not fully converted into **Mo3** could be expected from inspection of data in Figures 1 and 2. Indeed, the intensity of the pc2 wave, at which **Mo3** is produced, is significantly smaller than that of the one electron pc1 wave.

Preliminary DFT calculations were carried out to get insights into the reaction mechanism (Scheme 4, gas phase optimization PBE0-D3/Def2TZVP and solvent energy calculations (SMD, THF) at PBE0/Def2TZVP, see ESI for details). Relative energies were estimated using Cp*₂Co as a one electron reducing agent.



Scheme 4. DFT mechanism insights into reductive N₂ splitting with **Mo2**.

This choice has been motivated by the redox potential of Cp*₂Co⁺/Cp*₂Co (-1.84 V in THF, computed at -2.1 V) and the position of the reduction wave pc1 (-1.95 V vs. Fc⁺/Fc) are close. The lowest potential energy surface (PES) (lowest energy complexes with corresponding spin state) is presented. Complexes in different spin states have been computed and are

mentioned when relevant. Calculations start with the **Mo2** complex **4A**, a quartet of spin. One electron reduction leads to the anionic complex **5B** (quintet of spin) in a mildly exergonic process (-3.4 kcal mol⁻¹). Interestingly, one of the Mo-I apical bonds is strongly elongated in **5B** (5.38 Å), and thus the unsaturated complex **5C** [(PPP)MoI₂] lies close in energy (-0.6 kcal mol⁻¹ with

COMMUNICATION

respect to $^5\mathbf{B}$). Calculations could not locate a local extremum associated to N_2 coordinated to $^5\mathbf{C}$. As observed in the tri-iodide structure, octahedral geometry is not favored with a quintet spin state ($\text{Mo}\dots\text{N}_2$ distance of 4.45 Å). However, the complex $^3\mathbf{C}$ with a triplet spin state lies slightly above $^5\mathbf{C}$ (– 2.8 and – 4.0 kcal mol $^{-1}$ respectively) and coordination of N_2 to this complex is a kinetically facile step. Indeed, the transition state $\text{TS}(^3\mathbf{C}\text{--}^3\mathbf{D})$ is located only 15.9 kcal mol $^{-1}$ higher than $^3\mathbf{C}$. Dinitrogen Mo^{II} complex $^3\mathbf{D}$ is only 1.6 kcal mol $^{-1}$ higher than $^3\mathbf{C}$, and these two complexes are therefore in equilibrium. Splitting of N_2 was evaluated at the Mo^{II} redox state. Reaction between $^3\mathbf{C}$ and $^3\mathbf{D}$ to form a dimer $^3\mathbf{C}\text{--}\mathbf{D}$ (triplet spin state) or $^1\mathbf{C}\text{--}\mathbf{D}$ (singlet spin state) is computed to be endergonic with respect to $^3\mathbf{C}$ and $^3\mathbf{D}$ ($\Delta G = 9.6$ kcal mol $^{-1}$, $^1\mathbf{C}\text{--}\mathbf{D}$; $\Delta G = 4.9$ kcal mol $^{-1}$, $^3\mathbf{C}\text{--}\mathbf{D}$). Moreover, calculations of the transition states for N_2 cleavage for both dimers resulted in very high activation energies ($\Delta G^\ddagger = 52.0$ kcal mol $^{-1}$, from $^1\mathbf{C}\text{--}\mathbf{D}$; $\Delta G^\ddagger = 37.3$ kcal mol $^{-1}$, from $^3\mathbf{C}\text{--}\mathbf{D}$), and such pathway can be discarded.

One electron reduction of $^3\mathbf{C}$ and $^3\mathbf{D}$ is computed to be endoergic by $\Delta G = 5.4$ kcal mol $^{-1}$ and $\Delta G = 6.1$ kcal mol $^{-1}$, respectively. The reduced species are more stable as doublet spin states and iodide dissociation yields the mono-iodo complex [(PPP)MoI] ($^2\mathbf{E}$) and $^2\mathbf{F}$ from coordination to N_2 . The combined reduction / iodide dissociation is computed to be endoergic in the case of $^3\mathbf{C} \rightarrow ^2\mathbf{E} + \text{I}^-$ ($\Delta G = 4.3$ kcal mol $^{-1}$), whereas it is slightly exoergic in the case of $^3\mathbf{D} \rightarrow ^2\mathbf{F} + \text{I}^-$ ($\Delta G = -0.4$ kcal mol $^{-1}$). Contrary to the situation encountered with Mo^{II} center, the $\text{Mo}^{\text{I}}\text{--}\text{N}_2$ complex $^2\mathbf{F}$ is computed to be more stable than the unsaturated Mo^{I} complex $^2\mathbf{E}$ by $\Delta G = -3.1$ kcal mol $^{-1}$. As a result of this additional stability, the N_2 coordination to $^2\mathbf{E}$ is computed to be favorable ($\Delta G^\ddagger = 8.4$ kcal mol $^{-1}$) to yield $^2\mathbf{F}$. Formation of dimer species between $^2\mathbf{E}$ and $^2\mathbf{F}$, either as a singlet ($^1\mathbf{E}\text{--}\mathbf{F}$) or as a triplet ($^3\mathbf{E}\text{--}\mathbf{F}$) is computed to be exergonic ($\Delta G = -15.2$ kcal mol $^{-1}$, $^1\mathbf{E}\text{--}\mathbf{F}$; $\Delta G = -15.4$ kcal mol $^{-1}$, $^3\mathbf{E}\text{--}\mathbf{F}$). Despite being close in energy, the N_2 cleavage is operative only from the singlet dimer $^1\mathbf{E}\text{--}\mathbf{F}$ with an activation barrier of $\Delta G^\ddagger = 21.0$ kcal mol $^{-1}$, whereas the process is computed to be highly unfavorable from the triplet dimer ($\Delta G^\ddagger = 65.0$ kcal mol $^{-1}$). The singlet transition state exhibits an expected zig-zag geometry with a highly elongated N-N bond (1.631 Å vs. 1.192 Å in $^1\mathbf{E}\text{--}\mathbf{F}$) and shorter Mo-N contacts (1.689 Å and 1.693 Å vs. 1.868 Å and 1.871 Å in $^1\mathbf{E}\text{--}\mathbf{F}$). The overall transformation $^2\mathbf{E} + ^2\mathbf{F} \rightarrow 2\ ^1\mathbf{G}$, where $^1\mathbf{G}$ is the $\text{Mo}^{\text{IV}}\text{--}\text{nitrido}$ (Mo3) final product resulting from N_2 cleavage is computed to be strongly exoergic ($\Delta G = -55.3$ kcal mol $^{-1}$).

Overall, DFT studies support the electrochemical mechanism for N_2 splitting given in Scheme 3. It involves spontaneous iodide dissociation upon one-electron reduction to form the Mo^{I} di-iodide intermediate in equilibrium with the N_2 -coordinated Mo^{II} complex. Mo^{II} N_2 -dimer formation is thermodynamically accessible but N_2 cleavage is kinetically prohibited. A second reduction at more negative potential results in further iodide dissociation and easy N_2 coordination to Mo^{I} , resulting in thermodynamically easy formation of N_2 -dimer species from which splitting to Mo^{IV} nitride species is kinetically accessible.

In summary, we have demonstrated the electrochemical splitting of dinitrogen at a Mo molecular complex in ambient conditions, and characterized the formation of the corresponding Mo -nitride complex, which was obtained in 30% chemical yield (49%

Faradaic efficiency). Such nitride complexes are ideal starting point not only for the chemical functionalization but also and most importantly for electrochemical studies aiming at generating ammonia upon successive proton-coupled electron transfers (PCET process), one step closer from molecular electrochemical catalysis of N_2 reduction with metal complexes. Such studies will be reported in due time.

Acknowledgements

Authors would like to acknowledge support from the Agence Nationale de la Recherche (ANR) through the program ANR-16-CE07-0033-04. Partial financial support to M.R. from the Institut Universitaire de France (IUF) is gratefully acknowledged.

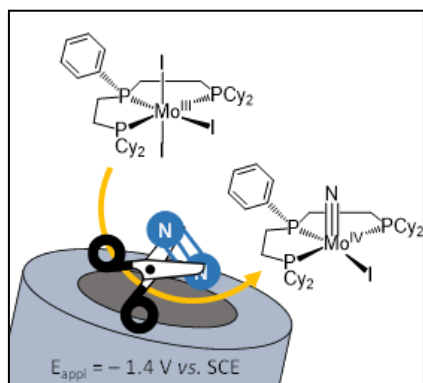
Keywords: Dinitrogen reductive splitting • electrochemical reduction of N_2 • molybdenum complex • nitride Mo complex

- [1] S. J. Ferguson, *Curr. Opin. Chem. Biol.* **1998**, *2*, 182–193.
- [2] N. Gruber, J. N. Galloway, *Nature* **2008**, *451*, 293–296.
- [3] J. Guo, P. Chen, *Chem* **2017**, *3*, 709–712.
- [4] R. Lan, J. T. S. Irvine, S. Tao, *Int. J. Hydrogen Energy* **2012**, *37*, 1482–1494.
- [5] B. M. Hoffman, D. Lukoyanov, Z. Y. Yang, D. R. Dean, L. C. Seefeldt, *Chem. Rev.* **2014**, *114*, 4041–4062.
- [6] D. V. Yandulov, R. R. Schrock, *Science (80-)*, **2003**, *301*, 76–78.
- [7] L. A. Wickramasinghe, T. Ogawa, R. R. Schrock, P. Müller, *J. Am. Chem. Soc.* **2017**, *139*, 9132–9135.
- [8] K. Arashiba, Y. Miyake, Y. Nishibayashi, *Nat. Chem.* **2011**, *3*, 120–125.
- [9] Y. Ashida, K. Arashiba, K. Nakajima, Y. Nishibayashi, *Nature* **2019**, *568*, 536–540.
- [10] Q. Liao, A. Cavaillé, N. Saffon-Merceron, N. Mézailles, *Angew. Chem. - Int. Ed.* **2016**, *55*, 11212–11216.
- [11] G. A. Silantsev, M. Förster, B. Schluschaß, J. Abbenseth, C. Würtele, C. Volkmann, M. C. Holthausen, S. Schneider, *Angew. Chem. - Int. Ed.* **2017**, *56*, 5872–5876.
- [12] A. S. Bennaamane, M. F. Espada, A. Mulas, T. Personeni, N. Saffon-merceron, M. Fustier-Boutignon, C. Bucher, N. Mézailles, *Angew. Chem. Int. Ed.* **2021**, *60*, 20210.
- [13] J. S. Anderson, J. Rittle, J. C. Peters, *Nature* **2013**, *501*, 84–87.
- [14] M. Reiners, D. Baabe, K. Münster, M. K. Zaretzke, M. Freytag, P. G. Jones, Y. Coppel, S. Bontemps, I. del Rosal, L. Maron, M. D. Walter, *Nat. Chem.* **2020**, *12*, 740–746.
- [15] R. B. Ferreira, B. J. Cook, B. J. Knight, V. J. Catalano, R. García-Serres, L. J. Murray, *ACS Catal.* **2018**, *8*, 7208–7212.
- [16] S. F. McWilliams, P. L. Holland, *Acc. Chem. Res.* **2015**, *48*, 2059–2065.
- [17] I. Klopsch, M. Finger, C. Würtele, B. Milde, D. B. Werz, S. Schneider, *J. Am. Chem. Soc.* **2014**, *136*, 6881–6883.
- [18] B. M. Lindley, R. S. Van Alten, M. Finger, F. Schendzielorz, C. Würtele, A. J. M. Miller, I. Siewert, S. Schneider, *J. Am. Chem. Soc.* **2018**, *140*, 7922–7935.
- [19] Q. J. Bruch, G. P. Connor, C. H. Chen, P. L. Holland, J. M. Mayer, F. Hasanayn, A. J. M. Miller, *J. Am. Chem. Soc.* **2019**, *141*, 20198–20208.
- [20] Y. Sekiguchi, K. Arashiba, H. Tanaka, A. Eizawa, K. Nakajima, K. Yoshizawa, Y. Nishibayashi, *Angew. Chem. Int. Ed.* **2018**, *57*, 9064–9068.
- [21] A. J. Kendall, S. I. Johnson, R. M. Bullock, M. T. Mock, *J. Am. Chem. Soc.* **2018**, *140*, 2528–2536.
- [22] T. Shima, J. Yang, G. Luo, Y. Luo, Z. Hou, *J. Am. Chem. Soc.* **2020**, *142*, 9007–9016.
- [23] A. J. Kendall, M. T. Mock, *Eur. J. Inorg. Chem.* **2020**, *2020*, 1358–1375.
- [24] S. Kuriyama, K. Arashiba, H. Tanaka, Y. Matsuo, K. Nakajima, K. Yoshizawa, Y. Nishibayashi, *Angew. Chem. Int. Ed.* **2016**, *55*, 14291–14295.

COMMUNICATION

- [25] T. Suzuki, K. Fujimoto, Y. Takemoto, Y. Wasada-Tsutsui, T. Ozawa, T. Inomata, M. D. Fryzuk, H. Masuda, *ACS Catal.* **2018**, *8*, 3011–3015.
- [26] L. R. Doyle, A. J. Wooles, L. C. Jenkins, F. Tuna, E. J. L. McInnes, S. T. Liddle, *Angew. Chem. Int. Ed.* **2018**, *57*, 6314–6318.
- [27] N. Ostermann, I. Siewert, *Curr. Opin. Electrochem.* **2019**, *15*, 97–101.
- [28] Q. J. Bruch, G. P. Connor, N. D. McMillion, A. S. Goldman, F. Hasanayn, P. L. Holland, A. J. M. Miller, *ACS Catal.* **2020**, *10*, 10826–10846.
- [29] M. J. Chalkley, M. W. Drover, J. C. Peters, *Chem. Rev.* **2020**, *120*, 5582–5636.
- [30] C. J. Pickett, J. Talarmin, *Nature* **1985**, *317*, 652–653.
- [31] E. Y. Jeong, C. Y. Yoo, C. H. Jung, J. H. Park, Y. C. Park, J. N. Kim, S. G. Oh, Y. Woo, H. C. Yoon, *ACS Sustain. Chem. Eng.* **2017**, *5*, 9662–9666.
- [32] T. J. Sherbow, E. J. Thompson, A. Arnold, R. I. Sayler, R. D. Britt, L. A. Berben, *Chem. - A Eur. J.* **2019**, *25*, 454–458.
- [33] T. J. Del Castillo, N. B. Thompson, J. C. Peters, *J. Am. Chem. Soc.* **2016**, *138*, 5341–5350.
- [34] P. Saha, S. Amanullah, A. Dey, *J. Am. Chem. Soc.* **2020**, *142*, 17312–17317.
- [35] P. Garrido-Barros, J. Derosa, M. Chalkley, J. Peters Tandem electrocatalytic N₂ fixation via concerted proton-electron transfer. ChemRxiv. Cambridge: Cambridge Open Engage; 2021; This content is a preprint and has not been peer-reviewed
- [36] R. S. van Alten, F. Wätjen, S. Demeshko, A. J. M. Miller, C. Würtele, I. Siewert, S. Schneider, *Eur. J. Inorg. Chem.* **2020**, *2020*, 1402–1410.
- [37] A. Katayama, T. Ohta, Y. Wasada-Tsutsui, T. Inomata, T. Ozawa, T. Ogura, H. Masuda, *Angew. Chem. Int. Ed.* **2019**, *58*, 11279–11284.
- [38] S. Bennaamane, M. F. Espada, I. Yagoub, N. Saffon-Merceron, N. Nebra, M. Fustier-Boutignon, E. Clot, N. Mézailles, *Eur. J. Inorg. Chem.* **2020**, *2020*, 1499–1505.
- [39] D. W. Meek, T. J. Mazanec, *Acc. Chem. Res.* **1981**, *14*, 266–274.

Entry for the Table of Contents



N₂ splitting was achieved with a simple Mo complex at a carbon electrode. Controlled reduction (3 electron transfer process) at -1.4 V vs. SCE and ambient conditions (room *T* and atmospheric *P*) afforded a Mo nitride complex in 30% yield. DFT studies support the transient formation of a Mo(I)-N₂-Mo(I) bridging dimer.

Institute and/or researcher Twitter usernames: ((optional))